Monthly Notices
of the
ROYAL ASTRONOMICAL SOCIETY

MNRAS **438,** 3049–3057 (2014)
Advance Access publication 2014 January 10

doi:10.1093/mnras/stt2411

How typical is the Coma cluster?

Kevin A. Pimbblet,[1,2,3,4★] Samantha J. Penny[2,3] and Roger L. Davies[4]

[1]*Department of Physics and Mathematics, University of Hull, Cottingham Road, Hull HU6 7RX, UK*
[2]*School of Physics, Monash University, Clayton, Victoria 3800, Australia*
[3]*Monash Centre for Astrophysics (MoCA), Monash University, Clayton, Victoria 3800, Australia*
[4]*Department of Physics, University of Oxford, Denys Wilkinson Building, Keble Road, Oxford OX1 3RH, UK*

Accepted 2013 December 12. Received 2013 December 11; in original form 2013 October 18

ABSTRACT

Coma is frequently used as the archetype $z \sim 0$ galaxy cluster to compare higher redshift work against. It is not clear, however, how representative the Coma cluster is for galaxy clusters of its mass or X-ray luminosity, and significantly, recent works have suggested that the galaxy population of Coma may be in some ways anomalous. In this work, we present a comparison of Coma to an X-ray-selected control sample of clusters. We show that although Coma is typical against the control sample in terms of its internal kinematics (sub-structure and velocity dispersion profile), it has a significantly high ($\sim 3\sigma$) X-ray temperature set against clusters of comparable mass. By de-redshifting our control sample cluster galaxies star formation rates using a fit to the galaxy main-sequence evolution at $z < 0.1$, we determine that the typical star formation rate of Coma galaxies as a function of mass is higher than for galaxies in our control sample at a confidence level of >99 per cent. One way to alleviate this discrepancy and bring Coma in line with the control sample would be to have the distance to Coma to be slightly lower, perhaps through a non-negligible peculiar velocity with respect to the Hubble expansion, but we do not regard this as likely given precision measurements using a variety of approaches. Therefore, in summary, we urge caution in using Coma as a $z \sim 0$ baseline cluster in galaxy evolution studies.

Key words: galaxies: clusters: general – galaxies: clusters: individual: Coma cluster – galaxies: evolution – X-rays: galaxies: clusters.

1 INTRODUCTION

Clusters of galaxies span a wide range of physical conditions and internal configurations. At the high-mass end of their mass distribution ($\sim 10^{15}$ solar masses), clusters may contain several thousand member galaxies that are orbiting with velocity dispersions over 1000 km s^{-1} (cf. Pimbblet et al. 2006; Ebeling et al. 2010). They are also rare celestial objects: they form from the gravitational collapse of extremely large perturbations within the primordial density field (e.g. Zel'Dovich 1970; Doroshkevich & Shandarin 1978) and continue to grow at all epochs through the accretion of fresh material; a large fraction of galaxies being funnelled directly to them through the filaments of the cosmic web (Pimbblet, Drinkwater & Hawkrigg 2004). From the point of view of studying galaxy evolution, clusters of galaxies offer excellent test beds as they contain a range of conditions from their outskirts (which may contain filaments and underdense 'void' regions that galaxies are being accreted from) through to high-density cores that contain a dense, hot (10^7–10^8 K) X-ray-emitting gas that is capable of stripping an infalling galaxy of its own star-forming gas (Gunn & Gott 1972; Cayatte et al. 1990; Quilis, Moore & Bower 2000; Boselli & Gavazzi 2006). Indeed, galaxies that are located at the centre of clusters (or high-density regions of the Universe) have long been noted to possess systematically different properties (star formation rates, colours, morphologies, masses) to those in low-density regions (e.g. Dressler 1980; Lewis et al. 2002; Gómez et al. 2003; Baldry et al. 2006; Bamford et al. 2009; Wilman & Erwin 2012, amongst many others). To address questions concerning the evolution of galaxies within these structures, samples of self-similar structures (and/or their likely progenitors) need to be assembled across cosmic time.

The Coma cluster (also known as Abell 1656 in the catalogue of Abell 1958) is the closest galaxy cluster of its mass (recently derived to be 1.8×10^{15} solar masses through a weak lensing analysis by Kubo et al. 2007) to us. This has led to Coma being extensively used as a redshift $z \approx 0$ baseline to compare higher redshift galaxy clusters to (e.g. Bahcall 1972; Mellier et al. 1988; Stanford, Eisenhardt & Dickinson 1995; Smith, Driver & Phillipps 1997; Kodama et al. 1998; Jørgensen et al. 1999; Jones, Smail & Couch 2000; Kodama & Bower 2001; van Dokkum et al. 2001; La Barbera et al. 2002; Rusin et al. 2003; De Lucia et al. 2004, 2007; Ellis & Jones 2004; Poggianti et al. 2004; Fritz et al. 2005; Holden et al. 2005;

★ E-mail: kevin.pimbblet@monash.edu

Moran et al. 2007; van Dokkum & van der Marel 2007; D'Onofrio et al. 2008; Giard et al. 2008; Ascaso et al. 2009; Bai et al. 2009; Lah et al. 2009; Stott et al. 2009).

Yet it is not clear how representative (or 'typical') the Coma cluster is for clusters of its mass. To illustrate this point, we note two recent examples. Stott et al. (2009) present an analysis of how the slope of the colour–magnitude relation (Visvanathan & Sandage 1977) of clusters varies with redshift. They find that the rest-frame slope evolves according to $(1 + z)^{1.77}$ (see their fig. 7). Yet, the slope for the Coma cluster lies at least 2σ away (steeper) from this relationship and its absolute value is much more in line with what might be expected of a $z \sim 0.3$ cluster (Stott et al. 2009). Indeed, the inclusion of Coma pulls their power-law fit upwards at the low-redshift end as it is the only point they consider at $z < 0.08$. Stott et al. (2009) attribute this mildly unusual slope to a lower than average dwarf-to-giant ratio along its red sequence (Stott et al. 2007) that suggests that it is still undergoing significant faint end evolution. Whilst Stott et al.'s result is likely not a statistically significant issue, other studies yield stronger issues with the use of Coma as a $z \approx 0$ baseline. Pertinent to this is the second example of Ascaso et al. (2009, see also Ascaso et al. 2008) who measure the structural properties (e.g. surface brightness profiles and quantitative galaxy morphologies) for a sample galaxies taken from five clusters at $0.18 < z < 0.25$ and compare them to Coma (using data from Aguerri et al. 2004). They find that the scales of the discs of late-type galaxies in the high-redshift clusters are significantly different to Coma. They offer two conclusions: either spiral galaxies have undergone a remarkable and very strong evolution over the past 2.5 Gyr, or 'Coma is in some way anomalous' (Ascaso et al. 2009).

Much earlier studies that concentrate on Coma itself describe the cluster as 'rich', 'regular' and (or) 'relaxed' (e.g. Kent & Gunn 1982 retain the assumption of the cluster being in equilibrium; see also Noonan 1961; Omer, Page & Wilson 1965, and references therein). Evidence subsequently accumulated that Coma was anything but a local archetype for relaxed and regular clusters: Henriksen & Mushotzky (1986) used X-ray observations to invalidate the assumption of an isothermal sphere (see also Johnson et al. 1979; Briel, Henry & Boehringer 1992; White, Briel & Henry 1993; Vikhlinin, Forman & Jones 1997; Neumann et al. 2003); the cluster contains multiple D-class galaxies (Beers & Geller 1983); and importantly the velocity distributions of the galaxy members themselves revealed sub-structure (Fitchett & Webster 1987; Merritt 1987; Mellier et al. 1988; Colless & Dunn 1996; Gambera et al. 1997; Edwards et al. 2002; Adami et al. 2009, see also Conselice & Gallagher 1998).

The central thesis of this work is to present a novel investigation of how typical the Coma cluster is in three well-defined and distinct ways that are well used in the literature. This comprises: (i) an investigation into the X-ray properties (particularly temperature and luminosity) of Coma in comparison to analogue clusters; (ii) a consideration of how kinematically perturbed or relaxed analogue clusters are to Coma; (iii) a determination of how 'active' – in the sense of star formation – the galaxies that make up analogous clusters are compared to Coma. The format for this work is as follows. In Section 2, we describe the creation of a set of control clusters that are analogous to Coma in mass from available Sloan Digital Sky Survey (SDSS) and X-ray data. We examine the X-ray properties of Coma in comparison to the control sample and an extended sample in Section 3. Section 4 deals with the kinematics of the galaxies contained in the clusters and in Section 5, we examine the star formation rates of the constituent galaxies in Coma and the control sample. Our results are summarized in Section 6. Throughout this work, we have used the Spergel et al. (2007) standard, flat cosmology in which $\Omega_{\rm M} = 0.238$, $\Omega_{\Lambda} = 0.762$ and $H_0 = 73$ km s^{-1} Mpc^{-1}.

2 DATA

We use two sets of data in this work, both taken from SDSS Data Release 7 (Abazajian et al. 2009). The first set of data is for the Coma cluster itself, whilst the second set (the control sample) consists of SDSS clusters that possess comparable X-ray luminosity (an observational proxy for mass since it originates from thermal Bremsstrahlung of the hot intra-cluster gas) to Coma. We make use of the SDSS value-added catalogues throughout this work, which includes star formation rates (Brinchmann et al. 2004) and masses (see www.mpa-garching.mpg.de/SDSS/DR7/Data/stellarmass.html).

To create the control sample, we note that Coma has an X-ray luminosity of $L_{\rm X} = 7.77 \times 10^{44}$ erg s^{-1} measured in the 0.1–2.4 keV band (Reiprich & Böhringer 2002). This level of emission is comparable with some of the most massive clusters in the Universe (cf. Ebeling, Edge & Henry 2001; Pimbblet et al. 2001). We therefore would like to select clusters with comparable $L_{\rm X}$ in the 0.1–2.4 keV band, but balance this with a need to have a sufficiently large control sample to contrast Coma against. We therefore select clusters within 5×10^{44} erg s^{-1} of Coma's X-ray luminosity. Since X-ray luminosity can predict cluster mass with an accuracy of >50 per cent, such a range is likely to correspond to no more than a factor of 2 range in mass from this $L_{\rm X}$ selection (Popesso et al. 2005). Secondly, we would like to select galaxy clusters to be at a comparable stage in their evolution as Coma. We first note that Kodama & Smail (2001) suggest the time-scale for galaxy morphological transformation within clusters may be as short as 1 Gyr if gas starvation effects are strong (see also Bekki, Couch & Shioya 2002; Moran et al. 2006; Tonnesen, Bryan & van Gorkom 2007; Boselli et al. 2008). Therefore, we wish to select clusters within a <1 Gyr look-back of Coma. This corresponds to a maximum redshift of $z \sim 0.08$ to select our clusters from.

We use the Base de Donnees Amas de Galaxies X (BAX) X-Ray Clusters Database (Sadat et al. 2004) to select clusters by using the above criteria. This yields a total of 47 clusters. Of these, one is Coma and a further 13 (30 per cent) are within the spatial limits of SDSS – this criterion of being within the observational bounds of SDSS is only applied after the X-ray selection within BAX. We detail the global properties of these clusters in Table 1, alongside Coma. We note that the clusters in the control sample have a mean $L_{\rm X} = 5.1 \pm 2.4 \times 10^{44}$ erg s^{-1} – only $\sim 1\sigma$ less than Coma's.

From this sample, we exclude NRGB045 on the grounds that it has an anomalously low-$T_{\rm X}$ value (0.83 keV). This is due to NRGB045 being more akin to a group than a cluster. Indeed, recent work by Stott et al. (2012) suggests that any galaxy grouping with $T_{\rm X} < 2$ keV would physically be considered a group rather than a bona fide cluster. The exclusion of NRGB045 from our subsequent analysis leaves us with 12 clusters in the control sample.

For each of the clusters in our control sample, we download all galaxies within 1 deg of the BAX-specified cluster centres from SDSS. For each cluster, we derive new estimates of their mean recession velocity ($\overline{cz}$) and velocity dispersion (σ_{cz}) from the 'gapping' technique of Zabludoff, Huchra & Geller (1990) and Zabludoff et al. (1993), which iteratively eliminates any galaxy from the computation of $\overline{cz}$ that is deviant by more than $3\sigma_{cz}$ from $\overline{cz}$. Errors on σ_{cz} are generated following Danese, de Zotti & di Tullio (1980). Although this method samples a factor of $\sim$2 different physical radii across our clusters (ranging from 2.2 Mpc for our lowest redshift

Table 1. The sample of clusters used in this work. The coordinates specify the Vizier position of the cluster. The X-ray luminosities in the 0.1–2.4 keV band (L_X) and temperatures (T_X) are sourced from BAX (Sadat et al. 2004) which is a compilation of X-ray data derived from many diverse literature sources. We cite the sources of these values below the table using parentheses next to each value. The virial radius (R_{virial}) is computed from σ_{cz}; see text for details. Bautz–Morgan (B–M) types have been sourced from NED except for the Zwicky clusters which we have determined ourselves.

Name	RA (J2000)	Dec. (J2000)	B–M Type	L_X ($\times 10^{44}$ erg s^{-1})	T_X (keV)	$\overline{cz}$ (km s^{-1})	σ_{cz} (km s^{-1})	Adopted R_{200} (Mpc)
Abell 85	00 41 38	−09 20 33	I	9.41[a]	$6.45^{+0.10}_{-0.10}$[d]	16 537 ± 58	898^{+45}_{-39}	1.80
Abell 119	00 56 21	−01 15 47	II–III	3.30[a]	$5.62^{+0.12}_{-0.12}$[e]	13 381 ± 56	917^{+43}_{-37}	1.83
Abell 660	08 25 22	+36 50 16	III	4.39[b]	N/A	19 647 ± 109	681^{+94}_{-66}	1.36
ZwCl 1215.1+0400	12 17 41	+03 39 32	II	5.17[a]	$6.54^{+0.21}_{-0.21}$[d]	23 109 ± 54	867^{+41}_{-36}	1.73
Abell 1775	13 41 56	+26 21 53	I	2.80[a]	$3.66^{+0.21}_{-0.12}$[f]	21 593 ± 113	1637^{+86}_{-74}	3.27
Abell 1795	13 49 01	+26 35 07	I	10.26[a]	$6.12^{+0.05}_{-0.05}$[d]	18 773 ± 55	719^{+42}_{-36}	1.44
Abell 1800	13 49 41	+28 04 08	II	2.89[a]	$4.14^{+0.09}_{-0.09}$[g]	22 915 ± 80	1018^{+61}_{-52}	2.04
ZwCl 1518.8+0747	15 21 52	+07 42 31	I	2.78[a]	$3.45^{+0.08}_{-0.06}$[f]	13 408 ± 88	1064^{+68}_{-57}	2.13
Abell 2061	15 21 15	+30 39 17	III	4.85[c]	$4.52^{+0.10}_{-0.10}$[g]	23 083 ± 52	841^{+39}_{-35}	1.63
Abell 2065	15 22 43	+27 43 21	III	5.55[a]	$5.44^{+0.09}_{-0.09}$[d]	22 213 ± 100	1887^{+75}_{-67}	3.77
Abell 2199	16 28 39	+39 33 06	I	4.09[a]	$3.99^{+0.10}_{-0.10}$[d]	9176 ± 44	761^{+33}_{-29}	1.52
Abell 2255	17 12 31	+64 05 33	II–III	5.54[a]	$5.92^{+0.24}_{-0.16}$[f]	24 071 ± 82	1223^{+62}_{-54}	2.45
Coma	12 59 49	+27 58 50	II	7.77[a]	$8.25^{+0.10}_{-0.10}$[h]	7166 ± 54	1639^{+40}_{-37}	3.28

[a]Reiprich & Böhringer (2002).
[b]Popesso et al. (2007a).
[c]Marini et al. (2004).
[d]Vikhlinin et al. (2009).
[e]Henry (2004).
[f]Ikebe et al. (2002).
[g]Shang & Scharf (2009).
[h]Arnaud et al. (2001).

cluster, Abell 2199, to 5.2 Mpc for ZwCl 1215.1+0400), the goal here is simply to provide an estimate of the redshift range to define a simple cluster membership criterion from within $3\sigma_{cz}$ of $\overline{cz}$. An analogous approach is taken for Coma, but using a 2 deg radius (a 3.4 Mpc radius). To place the clusters on to a common, physically meaningful scale, we limit our subsequent analysis to those galaxies to within $r_{200} \approx R_{Virial} = 0.002\sigma_{cz}$ (Girardi et al. 1998), where r_{200} is the clustocentric radius at which the mean interior density is 200 times the critical density; this value is well approximated by R_{virial}. Although we could compute this radii in other ways (e.g. Carlberg et al. 1997), we emphasize that this approximation is sufficient to serve to place our clusters on to a common scale. These values are tabulated in Table 1. Although it is known that there is considerable scatter in the L_X–σ_{cz} relationship (Popesso et al. 2005), the first conclusion to be drawn here is that Coma's velocity dispersion is not atypical compared to the control sample (which has a mean of 1043 ± 372 km s^{-1}), but is one of the largest given how we have selected the galaxy members. We point out that the control sample has a full range of Bautz & Morgan (1970) classifications (Table 1) – meaning that we cover a full range of galaxy cluster configurations and morphologies, ranging from those with obvious cD galaxies centrally located in the clusters to those lacking such a galaxy in entirety. Coma as a type II cluster that has two obvious, brightest cluster galaxies is not atypical against this control sample: we do not regard it as more dynamically evolved than the control sample.

3 X-RAY TEMPERATURE

From Table 1, it is already clear that Coma has the largest X-ray temperature (8.25 keV) out of all the comparable clusters selected within SDSS. The mean temperature of our control sample is $T_X = 5.1 \pm 1.1$ keV – some 2.9σ lower than the temperature of Coma. Such a large temperature means that the physical conditions inside Coma may actively regulate the star formation of galaxies contained therein. For example, Urquhart et al. (2010) note that high T_X clusters have a much lower fraction of photometrically blue galaxies (i.e. Butcher–Oemler fraction; Butcher & Oemler 1984) than low-T_X clusters and are highly unlikely to contain any extremely blue galaxies. Further, Popesso et al. (2007b) and Aguerri, Sánchez-Janssen & Muñoz-Tuñón (2007) find an anticorrelation between L_X and cluster blue fraction which supports this finding, given the scaling between L_X and T_X. This is reflected in the work of Poggianti et al. (2006) who demonstrate a broad anticorrelation between cluster velocity dispersion (a parameter that also scales with L_X; Davé, Katz & Weinberg 2002) and the fraction of star-forming cluster galaxies.

Popesso et al. (2005) report the scaling relationship between L_X and T_X in detail and show that there is both a trend and an appreciable scatter between the two variables (see also Davé et al. 2002). Although Coma's T_X value may be significantly larger than our control sample, we have used a factor of 2 range in L_X to draw this conclusion from. To determine if its T_X is truly anomalously

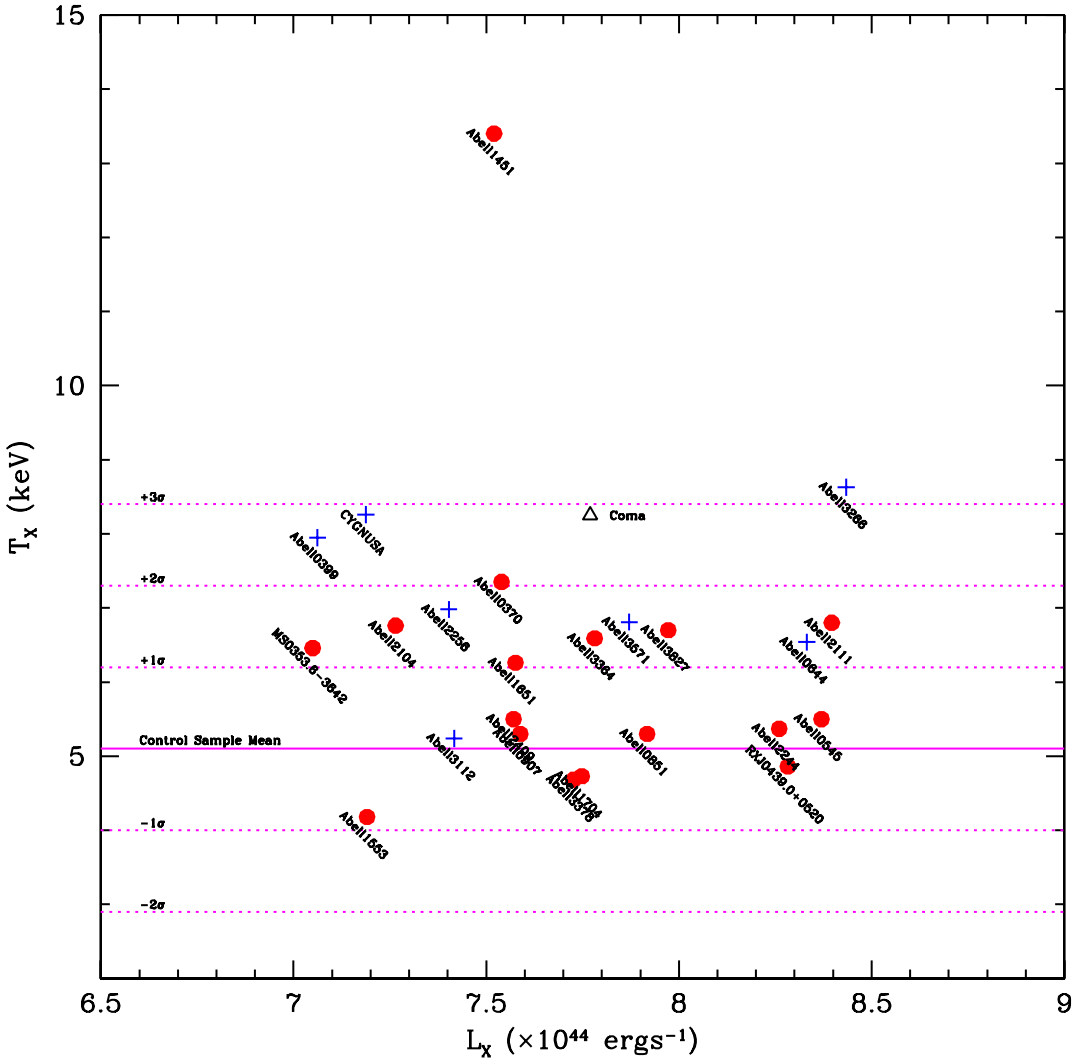

Figure 1. X-ray temperatures for clusters extracted from BAX within 1×10^{44} erg s^{-1} of Coma's X-ray luminosity that have T_X values available. Clusters below $z = 0.0814$ are marked with blue pluses, those above with red filled circles. Coma is marked by a triangle near the centre of the plot. The mean T_X of our control sample (i.e. those clusters inside the SDSS boundary that are within 5×10^{44} erg s^{-1} of Coma's X-ray luminosity) is denoted by the solid horizontal line and a few standard deviations either side of this are represented by the dotted lines, as labelled. Coma has one of the largest T_X values for this narrow L_X range and is $\sim 2.9\sigma$ above the control sample's mean T_X value.

high, we need to select clusters in a much narrower range of L_X. We turn again to BAX to do this and select *all* available clusters within 1×10^{44} erg s^{-1} of Coma's X-ray luminosity that also have a reliable X-ray temperature measurement available. In Fig. 1, we plot this narrow range of L_X against T_X for all available clusters. Coma is again seen to have one of the highest temperatures for all clusters in this range – both above and below the redshift cutoff of our control sample of $z = 0.0814$. But it is certainly within 2σ of the mean T_X of this narrower L_X range sample. That said, there is only one cluster either side of this redshift that has a larger X-ray temperature.[1]

We therefore conclude that Coma's X-ray temperature is comparatively high: both against our control sample and against all available clusters in a much narrower L_X range.

4 CLUSTER SUB-STRUCTURE

In this section, we address the second of our comparisons of Coma to the control sample using global cluster kinematical approaches. Depending on cosmological parameters, such as the matter density of the Universe, it might be expected that a rich cluster of galaxies (i.e. such as the ones that are in our sample) have perhaps had as much as half of their mass accreted within the past ∼few Gyr (e.g. Lacey & Cole 1993). Under such circumstance, it can be expected that a large fraction of rich clusters exhibit measurable sub-clustering. Coma is already well known to possess sub-clustering (see above). But, what fraction of our control sample also exhibits sub-clustering? To determine this fraction, we use the approach of Dressler & Shectman (1988, DS) to evaluate if the clusters possess significant sub-clustering. The test is powerful: Pinkney et al.

[1] We re-affirm the note made by Valtchanov et al. (2002) about Abell 1451 ($T_X = 13.4$ keV; Matsumoto et al. 2001) possessing a very significant deviation away from the L_X–T_X scaling relation (e.g. Popesso et al. 2005). This cluster merits future follow-up to discern the impact and potential cause of such an extreme temperature.

(1996) report that the DS approach is the most sensitive test for sub-clustering from a swathe of tests that they evaluated. The method works by computing a local mean local velocity ($\overline{cz}_{\rm local}$) and local velocity standard deviation ($\sigma_{\rm local}$) of a galaxy and its 10 nearest neighbours. These values are subsequently compared to the parent cluster's mean velocity and σ_z such that

$$\delta^2 = \left(\frac{N_{\rm local}+1}{\sigma_v^2}\right)[(\overline{cz}_{\rm local}-\overline{cz})^2+(\sigma_{\rm local}-\sigma_v)^2], \quad (1)$$

where δ is a measure of the deviation of the individual galaxy. The parameter of merit, Δ, is computed as the summation of all δ terms. This is contrasted with a Monte Carlo re-simulation of the cluster where the galaxy velocities have been randomly shuffled to each galaxy to generate $P(\Delta)$ and thereby estimate the confidence level that the cluster contains sub-structure.

Before we apply the DS test to our control sample, we need to not only use the cluster membership criterion derived above and limit the members to within $R_{\rm Virial}$, but also limit the cluster members to a similar absolute luminosity range and mass range. This is necessary since the sub-structure is strongly dependent on the galaxy luminosity range considered (Aguerri & Sánchez-Janssen 2010). This is achieved by considering the highest redshift cluster in the control group: Abell 2255. For this cluster, the SDSS limiting apparent magnitude of $r = 17.77$ corresponds to an absolute value of -19.85 (Fig. 2). At this limit, we are mass complete to log(stellar mass)=10.3 (Fig. 2). We subsequently impose these two limits in absolute magnitude and mass on all of our cluster members.

Due to a paucity of data (less than 30 galaxy members per cluster) after applying these cuts, we are forced to eliminate Abell 85, 660, 2199 and Zwicky 1518.8+0747 from our control sample at this stage. Of our sample, Abell 1775 and Abell 2065 (2 out of 8) produce a $P(\Delta)$ statistic that is <0.1 per cent (indicating certain sub-structure within $R_{\rm Virial}$). We note that this remains constant even if we ignore the absolute magnitude limit imposed above. Given the comparatively large velocity dispersion of these clusters, this is perhaps expected (Hou et al. 2012). Moreover, from ΛCDM simulations of clusters, Knebe & Müller (2000) demonstrate that some 30 per cent of all clusters should exhibit sub-clustering due to intercluster merger and infall activity (modulo slightly different selection criteria). We therefore regard Coma (and, indeed, our control group) as being 'typical' for clusters in a ΛCDM Universe for the level of sub-structure observed at our limits.

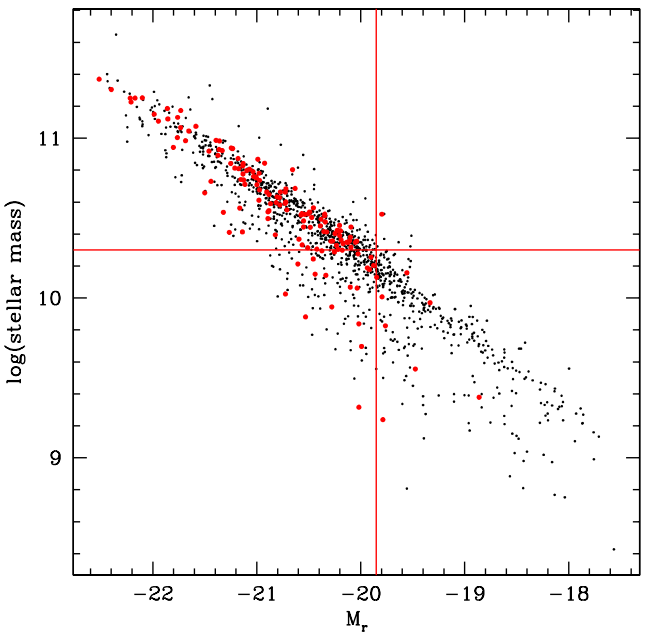

Figure 2. Mass and absolute luminosity of all galaxies in the control sample (smaller, black dots) with the contribution from the most distant cluster in our sample, Abell 2255, overlaid (larger, red dots). The SDSS limiting apparent magnitude of $r = 17.77$ is transformed into an absolute value using the mean redshift of Abell 2255 and denoted by the vertical line. The mass limit of log(stellar mass)=10.3 (horizontal line) denotes the mass above which we are complete for the sample. We apply these two criteria to the entire control sample to ensure we probe similar ranges in all clusters.

4.1 Velocity dispersion profiles

In recent years, a number of authors have probed how the velocity dispersion profile of clusters is affected by various cluster-intrinsic factors such as sub-structure (Hou et al. 2012) as well as potentially the dwarf-to-giant ratio (Pimbblet & Jensen 2012) and the occupancy of the cluster by different spectral classes of galaxy (Rood et al. 1972). To complement the above analysis, we now compute the velocity dispersion profile [$\sigma_{\rm P}(R)$] of each of our clusters following the prescription of Bergond et al. (2006, see also Hou et al. 2012). Formally,

$$\sigma_{\rm P}(R) = \sqrt{\frac{\sum_i w_i(R)(x_i-\overline{x})^2}{\sum_i w_i(R)}}, \quad (2)$$

where x_i are the measured radial velocities of each galaxy and $\overline{x}$ is the mean recession velocity of the cluster taken from Table 1. The weighting factors, w_i, are applied such that

$$w_i(R) = \frac{1}{\sigma_R}\exp\left(\frac{(R-R_i)^2}{2\sigma_R^2}\right), \quad (3)$$

where σ_R, the kernel width, is a free parameter that we arbitrarily set to $0.2R_{\rm Virial}$. The velocity dispersion profiles computed in this manner are displayed in Fig. 3. Interestingly, the clusters with

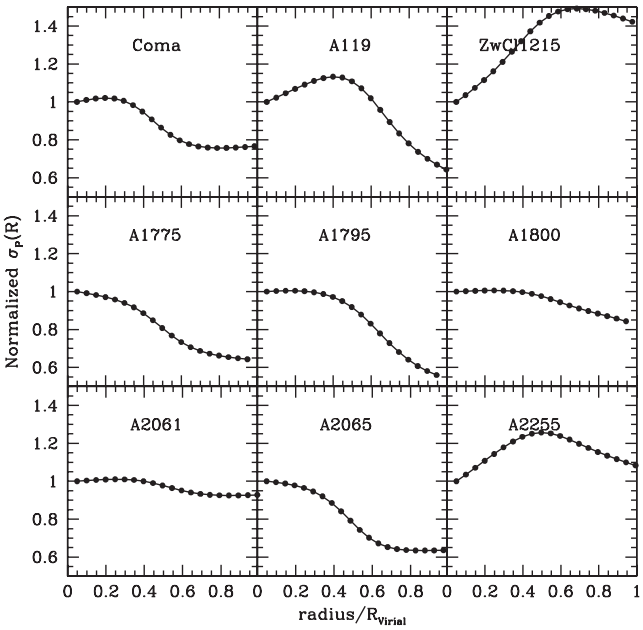

Figure 3. Velocity dispersion profiles of our clusters. For each cluster, $\sigma_{\rm P}(R)$ is normalized to the central value. ZwCl1215 (top right) is arguably the only cluster to display a strongly rising profile with radius whereas the other clusters either have a flat, falling or combination profile.

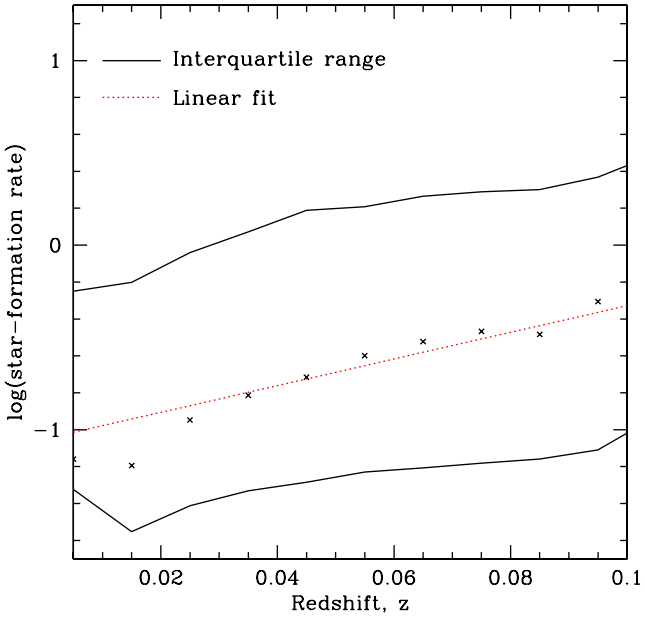

Figure 4. Evolution of the galaxy main sequence for log(stellar mass) = 10.4–10.6 SDSS galaxies up to $z = 0.1$. The points are the median star formation rates per redshift bin, whilst the solid lines give the interquartile range of the distribution. As noted by Noeske et al. (2007), the range of star formation also evolves with z. The linear fit (dotted line) to the data has a gradient of 7.22 ± 0.21, and we use this fit to evolve all the data in the control sample to Coma's redshift within the subsequent analysis.

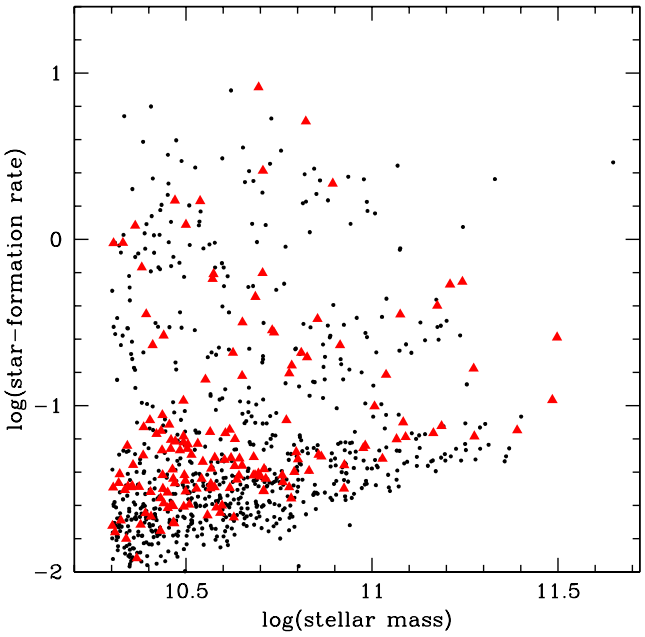

Figure 5. Galaxy main sequence for Coma (red triangles) versus the de-redshifted control sample (black dots). The galaxies in Coma have a higher systematic average star formation rate at a given stellar mass than the control sample.

significant sub-structure are not seen to have a rising velocity dispersion profile. This argues that any local kinematic group of galaxies may be at a late stage of homogenization with the wider cluster. This is in contrast to ZwCl 1215+0400 which does have a markedly rising profile and lack obvious sub-structure. This may be caused by multiple sub-clumps at large radii infalling for the first time. In comparison, Coma is quite unremarkably set against these profiles.

5 STAR FORMATION

In this section, we determine the star formation activity levels for cluster members in Coma and the control sample.

One way in which to do this is to use the galaxy main sequence (Noeske et al. 2007, and references therein): a plot of star formation rate against galaxy mass. This sequence is known to evolve with redshift – at high-z, the average star formation rate of galaxies is higher per galaxy mass than at lower z – the evolution in the trend being largely attributed to gas exhaustion. Therefore, if we are to use the galaxy main sequence to probe the activity levels in Coma and the control sample, we must first correct for this redshift evolution. We accomplish this by accessing all SDSS galaxies in 0.005 redshift bins up to $z = 0.1$, thereby encompassing all of our sample. For each bin, we compute the median and interquartile range of star formation rates[2] of log(stellar mass) = 10.4–10.6 galaxies (the choice of this mass range is arbitrary, but is sufficiently representative of our own sample and balances the need to have good statistics to compute the redshift evolution of the main sequence from). The results of this are displayed in Fig. 4. We fit the data with a linear relationship which has a gradient of 7.22 ± 0.21 in this range. Although the actual evolutionary relation will likely be of a higher order of $(1 + z)$, this linear relation is sufficient to describe these data at $z < 0.1$.

We use the gradient determined in Fig. 4 to de-redshift the star formation rates of galaxies in our control sample to that of Coma. In Fig. 5, we plot the galaxies from Coma and our de-redshifted control sample in the galaxy main-sequence phase space (again, using data from the value-added SDSS catalogue; Brinchmann et al. 2004). From this figure, we see that the galaxies in Coma appear to have a systematically higher star formation rate at a given stellar mass than the control sample.

But is this apparent observation real? A two-dimensional Kolmogorov–Smirnov (KS) test (Peacock 1983; Fasano & Franceschini 1987) returns a very low chance (<0.001 per cent; coupled with a high-Δ statistic) that the two distributions are drawn from the same sample. We therefore consider Coma to have a population whose galaxies possess significantly higher star formation rates on average than comparable clusters at similar evolutionary stages. We visually inspect those galaxies with very high star formation and specific star formation rates and confirm that they appear to be late-type (spiral and irregular) galaxies that we assume are undergoing a starburst phase.

A second way in which we may consider the active fraction is to use the divisor of McGee et al. (2011) who use log(specific star formation rate) = −11 to differentiate between active and passive galaxies. In Fig. 6, we plot the specific star formation rate of Coma galaxies and the de-redshifted control sample as a function of galaxy mass. The fraction of galaxies that are active by this definition are 0.09 ± 0.02 in Coma versus 0.14 ± 0.02 for the control sample. This is $\sim 2\sigma$ (depending on rounding) difference between the two samples. This appears to support (albeit at a weaker level) the inference of the two-dimensional KS test: the galaxies in Coma are systematically different to the control sample.

[2] Star formation rates for the galaxies are sourced from the SDSS value-added catalogue which are computed as per Brinchmann et al. (2004) using model fitting.

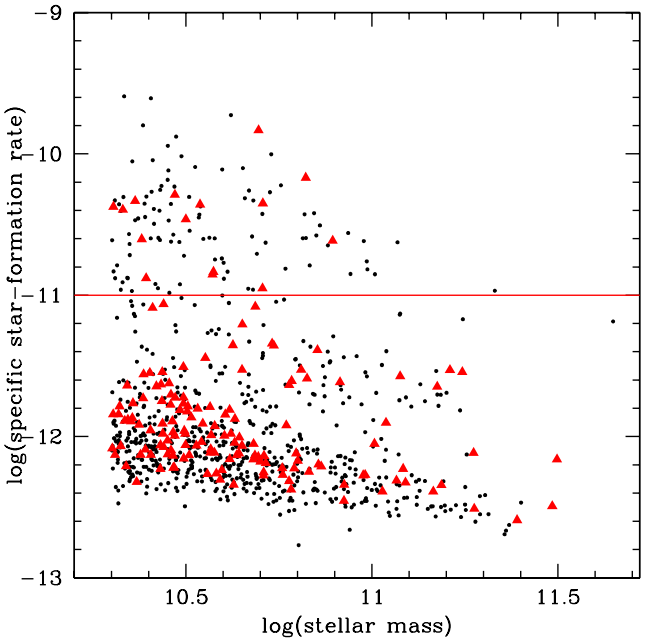

Figure 6. Specific star formation rates as a function of galaxy mass. Symbols are the same as per Fig. 5. The horizontal line denotes the McGee et al. (2011) delimiter between active (above the line) and passive (below the line) galaxies. The fraction of active galaxies differ between the two samples at a $\sim 2\sigma$ level.

6 DISCUSSION AND CONCLUSIONS

At the outset, we aimed to investigate three facets of Coma's galaxies in comparison to a control sample: an X-ray temperature and luminosity comparison, a kinematic comparison and a star formation activity comparison. One area that we have deliberately avoided is an examination of the luminosity function of Coma. This is on the grounds that it has already been well studied in comparison to other clusters at multiple wavelengths (recent examples include but are not limited to Adami et al. 2007; Cortese, Gavazzi & Boselli 2008; Bai et al. 2009; Yamanoi et al. 2012) and will likely follow the kinematic results for the control sample (in the sense that multiple components may be reflected in a superposition of functions; see also Tempel et al. 2009).

One way in which the situation of higher T_X coupled with higher star formation rate per galaxy mass bin being larger in Coma compared to the control sample might be arranged is if the bluer galaxies in Coma are just arriving into the cluster environment (given that a hotter intra-cluster medium should inhibit galaxy star formation subsequently). This ties with the Mahajan, Raychaudhury & Pimbblet (2012) finding: a high galaxy density in the infalling and filamentary regions of clusters such as Coma inevitably leads to a greater rate of galaxy–galaxy interaction and consequentially an increased starburst rate. But the problem with this interpretation is that there are ∼equally massive clusters in the control sample by design (i.e. the X-ray selection used here).

There have been hints in the literature that some of the special features of Coma might be alleviated if the distance to Coma was slightly lower. Consider, for example, fig. 6 of van Dokkum & van der Marel (2007) which shows that the mass-to-light ratio of Coma is similar to that of $z \sim 0.2$ clusters. If the distance to Coma were lower, then this ratio would increase, bringing Coma's mass-to-light ratio more in line with the trend observed with redshift by the same authors. This could be achieved if Coma had a non-negligible peculiar velocity with respect to the Hubble flow (e.g. towards the Shapley concentration). An interesting facet of this hypothetical change would be the driving of the star formation rates of Coma galaxies lower – bringing them more in line with the deredshifted control sample points. Given results that suggest Coma has been reported to have negligible peculiar velocity (e.g. Bernardi et al. 2002) and a variety of measurements agreeing within uncertainty on its distance (e.g. Capaccioli et al. 1990; D'Onofrio et al. 1997; Jensen, Tonry & Luppino 1999; Kavelaars et al. 2000; Liu & Graham 2001), we do not view this as a likely scenario; we supply it simply as an illustration.

In summary, in this work we have shown the following.

(i) Although Coma has a large velocity dispersion, it is not atypical for a cluster of its L_X. However, the X-ray temperature of Coma is rather high: some 2.9σ hotter than our control sample. Even considering all clusters available with a published T_X within 1×10^{44} erg s^{-1} of Coma reveals that it has one of the highest temperatures for all clusters in the range. Given the relationship between T_X and cluster galaxy properties, we urge strong caution in using Coma as a $z \sim 0$ baseline for studying cluster galaxy evolution.

(ii) Coma is well known to contain sub-structure. In comparison, we show that 2 out of 8 clusters in the control sample also contain significant sub-structure within $R_{\rm Virial}$. Coma is therefore unremarkable in this regard.

(iii) The velocity dispersion profiles of the control sample contain a mixture of rising, falling, flat and combination profiles. Coma is unremarkably set against this background and reinforces the above conclusion that Coma is kinematically normative for clusters of its ilk.

(iv) The general star formation rate of Coma cluster galaxies inferred from the galaxy main sequence is systematically higher than that for the control sample. A two-dimensional KS test rejects the hypothesis that the two samples are drawn from the same parent population with over 99 per cent confidence. Further, the fraction of actively star-forming galaxies by the definition of McGee et al. (2011) is 0.09 ± 0.02 for Coma versus 0.14 ± 0.02 for the control sample. We note in speculation that this discrepancy could be alleviated if the distance to Coma were smaller.

Thus, whilst Coma might be kinematically 'typical', the galaxies contained within are less suppressed in star formation rate than the comparison clusters. We consequentially urge caution in using Coma as a $z \sim 0$ cluster in galaxy evolution works: its galaxy population to the limits probed by this sample are not typical of clusters for its mass (as approximated by its X-ray luminosity).

ACKNOWLEDGEMENTS

KAP thanks Christ Church College, Oxford, for their hospitality whilst the bulk of this work was being undertaken. SJP is a Super Science Fellow at Monash University. KAP and SJP thank the Australian Research Council for their support through grant number FS110200047. We thank Ryan Houghton and Martin Bureau for valuable discussion during the preparation of this work.

We would like to express our gratitude to the anonymous referee for her/his robust feedback on the earlier versions of this manuscript.

This research has made use of the X-Ray Clusters Database (BAX) which is operated by the Laboratoire d'Astrophysique de Tarbes-Toulouse (LATT), under contract with the Centre National d'Etudes Spatiales (CNES).

Funding for the SDSS and SDSS-II has been provided by the Alfred P. Sloan Foundation, the Participating Institutions, the National

Science Foundation, the US Department of Energy, the National Aeronautics and Space Administration, the Japanese Monbukagakusho, the Max Planck Society and the Higher Education Funding Council for England. The SDSS website is http://www.sdss.org/.

The SDSS is managed by the Astrophysical Research Consortium for the Participating Institutions. The Participating Institutions are the American Museum of Natural History, Astrophysical Institute Potsdam, University of Basel, University of Cambridge, Case Western Reserve University, University of Chicago, Drexel University, Fermilab, the Institute for Advanced Study, the Japan Participation Group, Johns Hopkins University, the Joint Institute for Nuclear Astrophysics, the Kavli Institute for Particle Astrophysics and Cosmology, the Korean Scientist Group, the Chinese Academy of Sciences (LAMOST), Los Alamos National Laboratory, the Max-Planck-Institute for Astronomy (MPIA), the Max-Planck-Institute for Astrophysics (MPA), New Mexico State University, Ohio State University, University of Pittsburgh, University of Portsmouth, Princeton University, the United States Naval Observatory and the University of Washington.

This research has made use of the NASA/IPAC Extragalactic Database (NED) which is operated by the Jet Propulsion Laboratory, California Institute of Technology, under contract with the National Aeronautics and Space Administration.

REFERENCES

Abazajian K. N. et al., 2009, ApJS, 182, 543
Abell G. O., 1958, ApJS, 3, 211
Adami C., Durret F., Mazure A., Pelló R., Picat J. P., West M., Meneux B., 2007, A&A, 462, 411
Adami C. et al., 2009, A&A, 507, 1225
Aguerri J. A. L., Sánchez-Janssen R., 2010, A&A, 521, A28
Aguerri J. A. L., Iglesias-Paramo J., Vilchez J. M., Muñoz-Tuñón C., 2004, AJ, 127, 1344
Aguerri J. A. L., Sánchez-Janssen R., Muñoz-Tuñón C., 2007, A&A, 471, 17
Arnaud M. et al., 2001, A&A, 365, L67
Ascaso B., Moles M., Aguerri J. A. L., Sánchez-Janssen R., Varela J., 2008, A&A, 487, 453
Ascaso B., Aguerri J. A. L., Moles M., Sánchez-Janssen R., Bettoni D., 2009, A&A, 506, 1071
Bahcall N. A., 1972, AJ, 77, 550
Bai L., Rieke G. H., Rieke M. J., Christlein D., Zabludoff A. I., 2009, ApJ, 693, 1840
Baldry I. K., Balogh M. L., Bower R. G., Glazebrook K., Nichol R. C., Bamford S. P., Budavari T., 2006, MNRAS, 373, 469
Bamford S. P. et al., 2009, MNRAS, 393, 1324
Bautz L. P., Morgan W. W., 1970, ApJ, 162, L149
Beers T. C., Geller M. J., 1983, ApJ, 274, 491
Bekki K., Couch W. J., Shioya Y., 2002, ApJ, 577, 651
Bergond G., Zepf S. E., Romanowsky A. J., Sharples R. M., Rhode K. L., 2006, A&A, 448, 155
Bernardi M., Alonso M. V., da Costa L. N., Willmer C. N. A., Wegner G., Pellegrini P. S., Rité C., Maia M. A. G., 2002, AJ, 123, 2159
Boselli A., Gavazzi G., 2006, PASP, 118, 517
Boselli A., Boissier S., Cortese L., Gavazzi G., 2008, ApJ, 674, 742
Briel U. G., Henry J. P., Boehringer H., 1992, A&A, 259, L31
Brinchmann J., Charlot S., White S. D. M., Tremonti C., Kauffmann G., Heckman T., Brinkmann J., 2004, MNRAS, 351, 1151
Butcher H., Oemler A., Jr, 1984, ApJ, 285, 426
Capaccioli M., Cappellaro E., della Valle M., D'Onofrio M., Rosino L., Turatto M., 1990, ApJ, 350, 110
Carlberg R. G. et al., 1997, ApJ, 476, L7
Cayatte V., van Gorkom J. H., Balkowski C., Kotanyi C., 1990, AJ, 100, 604
Colless M., Dunn A. M., 1996, ApJ, 458, 435
Conselice C. J., Gallagher J. S., III, 1998, MNRAS, 297, L34
Cortese L., Gavazzi G., Boselli A., 2008, MNRAS, 390, 1282
D'Onofrio M., Capaccioli M., Zaggia S. R., Caon N., 1997, MNRAS, 289, 847
D'Onofrio M. et al., 2008, ApJ, 685, 875
Danese L., de Zotti G., di Tullio G., 1980, A&A, 82, 322
Davé R., Katz N., Weinberg D. H., 2002, ApJ, 579, 23
De Lucia G. et al., 2004, ApJ, 610, L77
De Lucia G. et al., 2007, MNRAS, 374, 809
Doroshkevich A. G., Shandarin S. F., 1978, MNRAS, 182, 27
Dressler A., 1980, ApJ, 236, 351
Dressler A., Shectman S. A., 1988, AJ, 95, 985 (DS)
Ebeling H., Edge A. C., Henry J. P., 2001, ApJ, 553, 668
Ebeling H., Edge A. C., Mantz A., Barrett E., Henry J. P., Ma C. J., van Speybroeck L., 2010, MNRAS, 407, 83
Edwards S. A., Colless M., Bridges T. J., Carter D., Mobasher B., Poggianti B. M., 2002, ApJ, 567, 178
Ellis S. C., Jones L. R., 2004, MNRAS, 348, 165
Fasano G., Franceschini A., 1987, MNRAS, 225, 155
Fitchett M., Webster R., 1987, ApJ, 317, 653
Fritz A., Ziegler B. L., Bower R. G., Smail I., Davies R. L., 2005, MNRAS, 358, 233
Gambera M., Pagliaro A., Antonuccio-Delogu V., Becciani U., 1997, ApJ, 488, 136
Giard M., Montier L., Pointecouteau E., Simmat E., 2008, A&A, 490, 547
Girardi M., Giuricin G., Mardirossian F., Mezzetti M., Boschin W., 1998, ApJ, 505, 74
Gómez P. L. et al., 2003, ApJ, 584, 210
Gunn J. E., Gott J. R., III, 1972, ApJ, 176, 1
Henriksen M. J., Mushotzky R. F., 1986, ApJ, 302, 287
Henry J. P., 2004, ApJ, 609, 603
Holden B. P. et al., 2005, ApJ, 626, 809
Hou A. et al., 2012, MNRAS, 421, 3594
Ikebe Y., Reiprich T. H., Böhringer H., Tanaka Y., Kitayama T., 2002, A&A, 383, 773
Jensen J. B., Tonry J. L., Luppino G. A., 1999, ApJ, 510, 71
Johnson M. W., Cruddace R. G., Fritz G., Shulman S., Friedman H., 1979, ApJ, 231, L45
Jones L., Smail I., Couch W. J., 2000, ApJ, 528, 118
Jørgensen I., Franx M., Hjorth J., van Dokkum P. G., 1999, MNRAS, 308, 833
Kavelaars J. J., Harris W. E., Hanes D. A., Hesser J. E., Pritchet C. J., 2000, ApJ, 533, 125
Kent S. M., Gunn J. E., 1982, AJ, 87, 945
Knebe A., Müller V., 2000, A&A, 354, 761
Kodama T., Bower R. G., 2001, MNRAS, 321, 18
Kodama T., Smail I., 2001, MNRAS, 326, 637
Kodama T., Arimoto N., Barger A. J., Arag'on-Salamanca A., 1998, A&A, 334, 99
Kubo J. M., Stebbins A., Annis J., Dell'Antonio I. P., Lin H., Khiabanian H., Frieman J. A., 2007, ApJ, 671, 1466
La Barbera F., Busarello G., Merluzzi P., Massarotti M., Capaccioli M., 2002, ApJ, 571, 790
Lacey C., Cole S., 1993, MNRAS, 262, 627
Lah P. et al., 2009, MNRAS, 399, 1447
Lewis I. et al., 2002, MNRAS, 334, 673
Liu M. C., Graham J. R., 2001, ApJ, 557, L31
Mahajan S., Raychaudhury S., Pimbblet K. A., 2012, MNRAS, 427, 1252
Marini F. et al., 2004, MNRAS, 353, 1219
Matsumoto H., Pierre M., Tsuru T. G., Davis D. S., 2001, A&A, 374, 28
McGee S. L., Balogh M. L., Wilman D. J., Bower R. G., Mulchaey J. S., Parker L. C., Oemler A., 2011, MNRAS, 413, 996
Mellier Y., Soucail G., Fort B., Mathez G., 1988, A&A, 199, 13
Merritt D., 1987, ApJ, 313, 121
Moran S. M., Ellis R. S., Treu T., Salim S., Rich R. M., Smith G. P., Kneib J.-P., 2006, ApJ, 641, L97
Moran S. M., Loh B. L., Ellis R. S., Treu T., Bundy K., MacArthur L. A., 2007, ApJ, 665, 1067

Neumann D. M., Lumb D. H., Pratt G. W., Briel U. G., 2003, A&A, 400, 811
Noeske K. G. et al., 2007, ApJ, 660, L43
Noonan T. W., 1961, PhD thesis, California Institute of Technology
Omer G. C., Jr, Page T. L., Wilson A. G., 1965, AJ, 70, 440
Peacock J. A., 1983, MNRAS, 202, 615
Pimbblet K. A., Jensen P. C., 2012, MNRAS, 426, 1632
Pimbblet K. A., Smail I., Edge A. C., Couch W. J., O'Hely E., Zabludoff A. I., 2001, MNRAS, 327, 588
Pimbblet K. A., Drinkwater M. J., Hawkrigg M. C., 2004, MNRAS, 354, L61
Pimbblet K. A., Smail I., Edge A. C., O'Hely E., Couch W. J., Zabludoff A. I., 2006, MNRAS, 366, 645
Pinkney J., Roettiger K., Burns J. O., Bird C. M., 1996, ApJS, 104, 1
Poggianti B. M., Bridges T. J., Komiyama Y., Yagi M., Carter D., Mobasher B., Okamura S., Kashikawa N., 2004, ApJ, 601, 197
Poggianti B. M. et al., 2006, ApJ, 642, 188
Popesso P., Biviano A., Böhringer H., Romaniello M., Voges W., 2005, A&A, 433, 431
Popesso P., Biviano A., Böhringer H., Romaniello M., 2007a, A&A, 461, 397
Popesso P., Biviano A., Romaniello M., Böhringer H., 2007b, A&A, 461, 411
Quilis V., Moore B., Bower R., 2000, Science, 288, 1617
Reiprich T. H., Böhringer H., 2002, ApJ, 567, 716
Rood H. J., Page T. L., Kintner E. C., King I. R., 1972, ApJ, 175, 627
Rusin D. et al., 2003, ApJ, 587, 143
Sadat R., Blanchard A., Kneib J.-P., Mathez G., Madore B., Mazzarella J. M., 2004, A&A, 424, 1097
Shang C., Scharf C., 2009, ApJ, 690, 879
Smith R. M., Driver S. P., Phillipps S., 1997, MNRAS, 287, 415
Spergel D. N. et al., 2007, ApJS, 170, 377
Stanford S. A., Eisenhardt P. R. M., Dickinson M., 1995, ApJ, 450, 512
Stott J. P., Smail I., Edge A. C., Ebeling H., Smith G. P., Kneib J.-P., Pimbblet K. A., 2007, ApJ, 661, 95
Stott J. P., Pimbblet K. A., Edge A. C., Smith G. P., Wardlow J. L., 2009, MNRAS, 394, 2098
Stott J. P. et al., 2012, MNRAS, 422, 2213
Tempel E., Einasto J., Einasto M., Saar E., Tago E., 2009, A&A, 495, 37
Tonnesen S., Bryan G. L., van Gorkom J. H., 2007, ApJ, 671, 1434
Urquhart S. A., Willis J. P., Hoekstra H., Pierre M., 2010, MNRAS, 406, 368
Valtchanov I., Murphy T., Pierre M., Hunstead R., Lémonon L., 2002, A&A, 392, 795
van Dokkum P. G., van der Marel R. P., 2007, ApJ, 655, 30
van Dokkum P. G., Stanford S. A., Holden B. P., Eisenhardt P. R., Dickinson M., Elston R., 2001, ApJ, 552, L101
Vikhlinin A., Forman W., Jones C., 1997, ApJ, 474, L7
Vikhlinin A. et al., 2009, ApJ, 692, 1033
Visvanathan N., Sandage A., 1977, ApJ, 216, 214
White S. D. M., Briel U. G., Henry J. P., 1993, MNRAS, 261, L8
Wilman D. J., Erwin P., 2012, ApJ, 746, 160
Yamanoi H. et al., 2012, AJ, 144, 40
Zabludoff A. I., Huchra J. P., Geller M. J., 1990, ApJS, 74, 1
Zabludoff A. I., Geller M. J., Huchra J. P., Vogeley M. S., 1993, AJ, 106, 1273
Zel'Dovich Y. B., 1970, A&A, 5, 84

This paper has been typeset from a TEX/LATEX file prepared by the author.